Downloaded from http://portlandpress.com/biochemi/article-pdf/doi/10.1042/BCJ20240338/961730/bcj-2024-0338.pdf by University of Missouri - Columbia user on 09 October 2024

Key structural role of a conserved cis-proline revealed by the P285S variant of soybean serine hydroxymethyltransferase 8

Vindya Samarakoon[†], Luckio F. Owuocha[£], Jamie Hammond[£], Melissa G. Mitchum[‡], and Lesa J. Beamer^{†£*}

†Department of Chemistry, University of Missouri, Columbia, MO 65211, USA

†Department of Biochemistry, University of Missouri, Columbia, MO 65211, USA

†Department of Plant Pathology and Institute of Plant Breeding, Genetics, and Genomics, University of Georgia, Athens, GA 30602, USA

*Corresponding author: Department of Biochemistry, University of Missouri, Columbia, MO 65211. Phone: (573) 882-6072. E-mail: beamerl@missouri.edu.

Abbreviations: cv., cultivar; FTHF, 5-formyl-THF; PDB, Protein Data Bank; PLP, pyridoxal 5-phosphate; SHMT, serine hydroxy-methyltransferase; SCN, soybean cyst nematode; THF, (6S)-tetrahydrofolate; TCEP, Tris(carboxyethyl)phosphine; RMSD, root mean square deviation

The enzyme serine hydroxymethyltransferase (SHMT) plays a key role in folate metabolism and is conserved in all kingdoms of life. SHMT is a pyridoxal 5'-phosphate (PLP) - dependent enzyme that catalyzes the conversion of L-serine and (6S)-tetrahydrofolate to glycine and 5,10methylene tetrahydrofolate. Crystal structures of multiple members of the SHMT family have shown that the enzyme has a single conserved cis proline, which is located near the active site. Here, we have characterized a Pro to Ser amino acid variant (P285S) that affects this conserved cis proline in soybean SHMT8. P285S was identified as one of a set of mutations that affect the resistance of soybean to the agricultural pathogen soybean cyst nematode. We find that replacement of Pro285 by serine eliminates PLP-mediated catalytic activity of SHMT8, reduces folate binding, decreases enzyme stability, and affects the dimer-tetramer ratio of the enzyme in solution. Crystal structures at 1.9 - 2.2 Å resolution reveal a local reordering of the polypeptide chain that extends an α-helix and shifts a turn region into the active site. This results in a dramatically perturbed PLP-binding pose, where the ring of the cofactor is flipped by ~180° with concomitant loss of conserved enzyme-PLP interactions. A nearby region of the polypeptide becomes disordered, evidenced by missing electron density for ~10 residues. These structural perturbations are consistent with the loss of enzyme activity and folate binding and underscore the important role of the Pro285 cis-peptide in SHMT structure and function.

Keywords: enzyme, enzyme mutation, enzyme structure, enzyme catalysis, structural biology, structure-function, X-ray crystallography, crystal structure

Serine hydroxymethyltransferase (SHMT) is a ubiquitous enzyme in eukaryotes, bacteria and archaea, and plays a key role in one-carbon folate metabolism. SHMT catalyzes the reversible conversion of L-serine to glycine while the hydroxymethyl group is transferred to (6S)-tetrahydrofolate (THF). THF is the carrier of one-carbon units used in the synthesis of purines, thymine nucleotides, and S-adenosyl methionine, the donor for many methyl group transfers. The reaction of SHMT is dependent on the cofactor pyridoxal 5'-phopshate (PLP), which is covalently attached through a Schiff base to an active site lysine in the resting state of the enzyme. Due to their roles in one-carbon metabolism, enzymes in the SHMT family are targets for the design of antibacterial [1, 2], antimalarial [3–6], herbicides [7, 8], and chemotherapeutic agents [9–13].

We have previously characterized the 3D structure and activity of a cytoplasmic isoform of SHMT from soybean (*Glycine max*), designated as SHMT8 [14, 15]. Two amino acid polymorphisms of SHMT8 from the soybean cultivar (cv.) Forrest are linked to increased resistance to the soybean cyst nematode (SCN), relative to the SCN-susceptible soybean cv. Essex. SCN is a devastating agricultural pathogen responsible for more than a billion-dollar loss in crop damage in the U.S. annually [16]. Mutants of Forrest SHMT8 have been identified in soybean that show intermediate effects on SCN resistance between that of cv. Essex and cv. Forrest [17, 18]. The effects of these mutations on enzyme structure and activity have not been experimentally characterized. An understanding of their biochemical phenotypes may provide new insights into the properties of SHMT8 that affect SCN resistance.

In this study, we investigate one of the previously identified variants of Forrest SHMT8: a point mutation of Pro285 to serine (P285S) identified in soybean line F650 [17]. Previous crystal structures of soybean SHMT8 [14] show that Pro285 is adjacent to both the PLP and THF-binding sites of the enzyme (Figure 1A). Pro285 also participates in the sole cis-peptide bond in the polypeptide chain of SHMT8 (471 amino acids). Cis-peptides (Figure 1B) are generally quite rare in protein structures (<0.05%), although cis peptides between proline and a preceding residue are somewhat more common (~5%) due to the unique geometry of the proline side chain [19, 20]. Cis-prolines are often conserved in protein families, consistent with important roles in structure and function [19–21].

Here we characterize the biochemical and structural impacts of the P285S variant of soybean SHMT8. Despite the relatively conservative Pro → Ser substitution, widespread impacts on protein structure occur related to the loss of the cis-peptide conformation at Ser285. Structural changes involve both local and propagated rearrangements, as well as perturbation of the PLP-binding pose. Biochemical effects, including the elimination of PLP-mediated catalysis and a decrease in enzyme stability, mirror the structural impacts. This work provides new insights into the PLP binding site of SHMT and defines a key role for this cis proline in SHMT structure and function.

Results

Overview of the conserved cis proline in the SHMT enzyme family

Downloaded from http://portlandpress.com/biochem/article-pdfldoi/10.1042/BCJ20240338/961730/bcj-2024-0338.pdf by University of Missouri - Columbia user on 09 October 2024

The SHMT enzyme family is widespread in evolution and structurally conserved. The enzyme typically exists as a dimer in prokaryotes or tetramer in eukaryotes. The tetramer is composed of two obligate dimers, each formed by two tightly intertwined protomers (Figure 1A, 2A). Each obligate dimer has two active sites comprised of residues from both polypeptide chains, which make numerous contacts with ligands (Figure 1C). The PLP binding site is deeply buried and adjacent to the interface of the two polypeptide chains in the obligate dimer. The substrate tetrahydrofolate binds nearby, in an extended tunnel that leads to the surface of the enzyme (Figure 2). Both binding sites are highly conserved in sequence and structure within the SHMT family. A detailed analysis of residues involved in the SHMT8 active site may be found in [14].

Among the 450+ residues in the typical SHMT protomer, which includes 24 prolines in SHMT8, only one has a peptide bond in the cis conformation. In soybean SHMT8, this occurs between Phe284 and Pro285. Previous crystal structures of SHMT8 in complex with various ligands show that Pro285 is found at the C-terminus of an α -helix and is adjacent to both the folate and PLP-binding sites (Figure 2). Because of the highly intertwined nature of the SHMT obligate dimer, Pro285 of chain A is closest to the PLP bound to chain B, and vice versa. The Pro285 side chain is sandwiched between two phenylalanine rings from residues 281 and 284 (Supplementary Figure 1). Together, these three hydrophobic residues line one wall of the folate binding tunnel of the enzyme. The residue following Pro285 is Ser286, which is involved in multiple contacts with the alternate polypeptide chain in the obligate dimer.

A proline at the residue position corresponding to Pro285 of soybean SHMT8 is highly conserved in the SHMT enzyme family. An alignment of 73 sequences of SHMT structures currently available in the Protein Data Bank (PDB) (overall sequence identities ranging from 34

to 94%) shows that proline is completely conserved at this position (Supplementary Figures 2,3). With only a few exceptions, the corresponding proline has a cis-peptide bond (Supplementary Figure 1). The sequence and structural conservation of this cis-proline in the SHMT family, along with its location near the enzyme active site, is indicative of potential functional importance, as has been seen in other enzyme systems [19–21].

The P285S substitution causes structural rearrangements of the protein and perturbation of PLP-binding

For structural and biochemical studies, the P285S variant of SHMT8 was prepared in both the Essex and Forrest SHMT8 sequence backgrounds, which we refer to as E.P285S and F.P285S, respectively. Forrest SHMT8 differs from Essex SHMT8 at two amino acid positions: P130R/N358Y [18]. Characterization of both E.P285S and F.P285S allows assessment of the impacts of the P285S variant on SHMT8 structure and function separate from those of the P130R/N358Y polymorphisms, which greatly impair folate-binding by Forrest SHMT8 [14]. Overall, Essex and Forrest SHMT8 are quite similar in 3D structure with the exception of a loop near the entrance of the folate binding site, which shows reduced flexibility in Forrest SHMT8 and impedes folate binding [14].

Crystal structures of E.P285S and F.P285S were determined at resolutions of 2.25 and 1.90 Å, respectively (Materials and Methods; Table 1). In both cases, the P285S variants adopt the conserved tetrameric assembly found in the Essex and Forrest SHMT8 structures [14]. Both E.P285S and F.P285S have PLP covalently attached to Lys244 as an internal aldimine in all chains (Figure 3A), although electron density maps for the ligand are clearer for F.P285S

(Supplementary Figure 4). However, beyond these overall similarities with previous structures, significant changes associated with the serine substitution are observed, including a dramatic reorientation of the PLP binding pose, local and longer-range rearrangements of the polypeptide chain, and a new region of induced structural disorder. The known Essex and Forrest SHMT8 complexes with PLP (PDB ID 6UXH and 6UXK) or the PLP-glycine (PLP-Gly) external aldimine intermediate (PDB ID 6UXI and 6UXL) provide a basis for detailed comparisons of the P285S variants. For the following analyses, chains A of E.P285S and F.P285S are used, unless otherwise stated. (Some small variations in the regions of conformeric change and numbers of disordered residues are found in other chains in the asymmetric unit.)

Examination of the site of mutation shows that substitution of Pro285 with serine results in loss of the cis-peptide bond involving this residue. In both E.PS85S and F.P285S, the peptide bond between Phe284 and Ser285 adopts a trans conformation, extending the α -helix that previously terminated at Pro285. This helix extension shifts a turn region (residues 287-289) into the binding site of PLP, near the phosphate group (Figure 3B), blocking the standard binding orientation of the cofactor. As a result, the PLP ring flips by ~180° such the phosphate group is on the opposite side of the binding site, and tilts approximately 40° out of its usual plane (compare PLP in yellow vs. orange in Figure 3B). An animation illustrating the structural differences produced by the P285S variant may be found in Supplementary file S1.

The remarkable change in binding pose of the PLP in the E.PS85S and F.P285S variants eliminates all the standard enzyme-cofactor interactions, while several new interactions are seen. Specifically, the reorientation of PLP places the phosphate group of the cofactor in the approximate position of the glycine moiety observed in SHMT8 complexes with the PLP-Gly external aldimine (Figure 3C). Complexes of soybean SHMT8 bound to PLP-Gly - an

intermediate in the SHMT reaction - have been previously characterized (PDB IDs 6UXI and 6UXL, respectively)[14]. Through comparisons with these structures, it can be seen that Arg389 and Tyr59, both of which have roles in binding PLP-Gly (Figure 3C), make alternative contacts to the phosphate group of PLP in its perturbed binding pose caused by the P285S mutation (Figure 3D). One of these is direct – a salt bridge with Arg389 – while Tyr59 makes a water-mediated interaction to the phosphate group. While these contacts are almost certainly adventitious, the ability of the enzyme to accommodate PLP in its perturbed orientation appears be related to its large and complex active site, which utilizes two substrates (Gly and folate) and the PLP cofactor at various points in its multi-step reaction.

In addition to the local perturbations of protein structure and altered binding of PLP, both P285S variants exhibit longer range structural changes, as well as an increase in the number of disordered residues (i.e., no longer visible in electron density maps). The most significant conformational change occurs between residues 128-147, which contains a previously described "tetramer interface loop" of SHMT8 [15]. Due to steric conflicts with the altered binding pose of PLP, parts of this region adopt a new conformation while other residues become disordered (132-143) (Figure 3A). One consequence of these changes is a significant reduction from \sim 1500 Å² to 700 Å² in the contact surface between the two obligate dimers in the SHMT8 tetramer (Supplementary Figure 5).

The P285S substitution causes loss of PLP-mediated catalysis and reduced folate binding affinity

The observed structural impacts of the P285S variant suggested possible changes to enzyme function. The PLP-mediated activity of the E.P285S and F.P285S variants was assessed

by monitoring the retro-aldol cleavage of the β-hydroxy-amino acid L-phenylserine to benzaldehyde. This assay is independent of folate and both Essex and Forrest SHMT8 are highly active in this assay [14]. In contrast, both E.P285S and F.P285S lack measurable activity (Supplementary Figure 6 A,B). This result is consistent with the altered PLP binding pose observed in the P285S crystal structures.

To investigate the effect of the P285S variant on folate binding affinity, we determined binding constants in a two-substrate system that exploits a spectrophotometrically observable change associated with folate binding [22]. For this assay, 5-formyl-THF (FTHF) is used instead of THF, because of its increased solubility and stability in solution. Our previous studies showed that Essex SHMT8 binds FTHF with a K_d of 17 μ M, while Forrest SHMT8 has greatly impaired folate binding activity [14]. In the case of the P285S substitution, both E.P285S and F.P285S are found to lack measurable folate binding activity (Supplementary Figure 6 C, D). Impaired folate binding for F.P285S was expected, given that the P130R/N258Y polymorphisms in Forrest SHMT8 are sufficient to eliminate measurable folate binding [14]. Loss of FTHF binding by E.P285S presumably reflects the proximity of the serine mutation to the folate binding pocket of the enzyme and the resulting structural impacts (Figures 2 and 3).

The P285S substitution decreases stability of the SHMT8 tetramer

To assess the impacts of the P285S variant on the oligomeric state of SHMT8, we used native polyacrylamide gel electrophoresis. With this method, both Essex and Forrest SHMT8 migrate primarily as tetramers on native gels (Figure 4A). This is generally consistent with previous studies from SAXS and AUC that showed tetramers in solution [14], although the

native gels indicate some dimer for Forrest SHMT. In contrast, both the E.P285S and F.P285S variants have a marked increase in the relative amount of dimer, compared to their counterparts with Pro285. This is particularly true for F.P285S, which appears to have roughly a 1:1 ratio of dimer:tetramer on the native gel. [Note: some bands of unknown origin with apparent higher molecular weight (MW) are also present, but are not seen on SDS page gels (Figure 4B,C)]. Size exclusion chromatography profiles (Supplementary Figure 7) also suggest a mix of tetramer and dimer for E.P285S, consistent with the native gels.

The reduction in tetramer formation of the P285S variants is consistent with the structural changes associated with the serine substitution, particularly in the region of the tetramer interface loop (Figure 3A) and the resulting reduction in surface area of the interface between obligate dimers. The alteration in PLP binding observed in the crystal structures may also be a factor, as reduced stability of the SHMT tetramer in the absence of PLP is known for other eukaryotic members of the SHMT family [11, 23–25].

The P285S substitution increases protein flexibility and reduces thermal stability

Limited proteolysis by proteinase K was used to evaluate potential differences in protein flexibility and/or structural disorder of the P285S variants. For comparison, Essex and Forrest SHMT8 were also characterized (Figure 4B, C). Some differences in the patterns of proteolytic digestion are apparent between Essex and Forrest SHMT8, with the latter having additional lower MW bands early in the time course of digestion, presumably related to the P130R/N285Y double amino acid polymorphism. Both the E.P285S and F.P285S variants show changes in proteolytic cleavage, including a general increase in susceptibility, novel sites of cleavage and

more rapid degradation. These differences are consistent with the altered conformations and locally unstructured regions observed in the crystal structures of the P285S variants.

We also measured stability of the P285S variants to thermal denaturation by circular dichroism (CD) (Supplementary Figure 8). Consistent with previous studies [15], we find Essex SHMT8 to be more stable (T_m = 59 °C) than Forrest SHMT8 (T_m = 53 °C) by ~6 °C. Introduction of the P285S variant further decreases stability, with a T_m for E.P285S of 52 °C and T_m for F.P285S of 49 °C, reductions of 7° and 4 °C, respectively.

Discussion

The P285S variant of SHMT8 was identified in ethyl methanesulfonate mutagenized populations of soybean cv. Forrest selected for reduced resistance to SCN [17]. Although the P285S variant was not further characterized, several other mutants of SHMT8 identified in the same study were inactive in *E. coli* complementation assays, suggesting that lack of enzyme activity was associated with partial loss of SCN resistance. Our results here show that the P285S variant is also functionally impaired, notably in PLP-mediated catalysis and folate binding, and also exhibits reduced stability of the tetramer and thermal stability of the enzyme. The association of these biochemical deficits with a reduction in SCN resistance remains to be elucidated, but the reduction in oligomeric stability characterized herein raises the possibility of dominant negative effects through subunit exchange, such as with SHMT5, an alternative isoform also found the soybean cytoplasm [26]. Ongoing studies of other SHMT8 mutants identified in [17] may help provide further insights.

Downloaded from http://portlandpress.com/biochemi/article-pdf/doi/10.1042/BCJ20240338/961730/bcj-2024-0338.pdf by University of Missouri - Columbia user on 09 October 2024

Our biochemical and structural characterizations of the P285S variant establishes key functional and structural roles for this cis-proline in the SHMT enzyme family. The substitution of serine for proline has widespread impacts related to loss of the cis-peptide bond between Phe284 and Pro285. Both local and long-range changes to the polypeptide chain as well as a dramatic reorientation of the PLP cofactor are observed. Impacts on enzyme function and oligomeric state are also significant. Moreover, sequence and structural conservation of this cis-proline indicate its importance likely extends to the entire SHMT family. This reaffirms the previously noted connections between cis-prolines and regions of functional importance in other proteins [19–21].

The conserved cis-proline of SHMT was previously noted to have a role in folding pathway of the enzyme. An investigation of proline residues in the folding of *Escherichia coli* SHMT (45% sequence identity to soybean SHMT8) identified mutations of the corresponding cis-proline (Pro258) and another nearby proline (Pro264) as affecting folding kinetics and reducing catalytic activity [27]. The *E. coli* Pro258 mutants also show reduced thermal stability, as seen in the soybean variant. In *E. coli* SHMT, Pro258 and Pro264 are found within a 50-residue "interdomain" segment involved in the final, slow phase of protein folding and the formation of the holo-enzyme (i.e., covalent attachment of PLP). In our crystal structures of the P285S variants, the equivalent proline residues flank the loop region that changes conformation and protrudes into the PLP-binding site of SHMT8. The correspondence of this structurally perturbed loop to a segment of the polypeptide chain that gains structure late in the folding pathway may help explain how SHMT8 is able to maintain its overall fold and oligomeric assembly, despite the substantial detrimental impacts of the P285S mutation.

Enzymes in the SHMT family exhibit complex interrelationships among activity, stability, and oligomeric state [23–25]. These connections are consistent with the multiple, simultaneous perturbations observed in the P285S variant of soybean SHMT8. Among these, the dramatic change in the binding pose of the PLP cofactor is perhaps most notable, given the highly conserved nature of the PLP-binding site and its deeply buried location in the enzyme. To our knowledge, similar dramatic alterations of PLP-binding have not previously been observed despite many studies of enzymes that utilize PLP as a cofactor. The widespread effects of the dysfunctional P285S variant on enzyme structure and function may have relevance to understanding other genetic mutations of SHMT, including those involved in human inherited disease [28, 29].

Materials and Methods

Enzyme expression, purification, and crystallization

The SHMT8 variants P285S of Essex and Forrest SHMT8 were commercially prepared (GenScript) in a pET-14b expression vector with an N-terminal His₆-affinity tag and recombinantly expressed in *Escherichia coli* BL21(DE3). Cell cultures were grown in terrific broth supplemented with 50 µg mL⁻¹ ampicillin and protein expression was otherwise performed as previously described [14].

Cell pellets were resuspended in lysis buffer containing 50 mM HEPES, pH 7.5, 300 mM NaCl, 10 mM imidazole, 5% (v/v) glycerol, 1% Tween 20, and 1 mM PLP, sonicated, and centrifuged at 16,500 rpm for 1 h at 4 °C. The supernatant was loaded onto a Ni-NTA agarose

column (Qiagen). The column was washed with 40 mL of lysis buffer and the protein was eluted with 50 mM HEPES, pH 7.5, 300 mM NaCl, 300 mM imidazole, 3.5% (v/v) glycerol. The elute was dialyzed in 50 mM HEPES, 150 mM NaCl, 0.5 mM Tris(2-carboxyethyl) phosphine (TCEP) and 2% glycerol to remove imidazole. The dialyzed protein was concentrated to 24 mg mL⁻¹, flashed frozen in liquid nitrogen and stored in -80 °C.

Initial crystallization screens were set up at 19 °C using the sitting drop vapor diffusion method and crystal screen kits INDEX (HR2-144) and PEG/Ion 2 screen (HR2-098) (Hampton Research) at a protein concentration of 12 mg/mL. PLP was added to each protein before crystallization at 0.12 mM. Screens were also conducted in the absence and presence of glycine (40 mM) and FTHF (6 mM) to encourage potential ligand complexes. However, no ligands other than the PLP internal aldimine with Lys244 were observed in either structure. Drops containing 2 μl of the protein-ligand solution and 2 μl crystallization buffer were sealed over a 0.1 mL reservoir. Data collection quality crystals for both P285S variants were obtained in 2% (v/v) Tacsimate, pH 7.0, 0.1 M HEPES, pH 7.5, and 20% (w/v) polyethylene glycol 3,350. Crystals were cryoprotected by 25% ethylene glycol and flash cooled in liquid nitrogen.

X-ray diffraction data collection, phasing, and refinement

X-ray diffraction data were collected at Advanced Light Source beamline 4.2.2 using a Taurus-1 CMOS detector. Datasets were integrated and scaled with XDS [30], and intensities were merged and converted to amplitudes with Aimless [31]. Phases for the P285S variant structures were determined by molecular replacement using Phaser as implemented in PHENIX [32] and the Essex SHMT8•PLP coordinates (PDB ID: 6UXH). Model building and refinement

were carried out in COOT [33] and PHENIX [32], respectively. Residue 244 was modeled as mixture of lysine and Lys-PLP, with the latter at occupancies ranging from 0.75 to 0.85 depending on the structure and chain. Structural figures were produced using PyMol [34] unless otherwise noted. Surface area of the protein interfaces was calculated by PISA [35].

Kinetic and ligand binding assays

DL-phenylserine (Millipore-Sigma) was used as a substrate to determine kinetic parameters for the folate-independent retro-aldol cleavage [15]. Reactions were carried out in a buffer containing 25 mM HEPES (pH 7.5), 50 mM NaCl, and 0.5 mM TCEP in an Epoch II plate reader (BioTek). Each reaction contained 4 μM protein and 1 – 250 mM DL-phenylserine. Benzaldehyde formation was monitored at 279 nm. The initial slopes of the reactions were used to determine enzyme activity, and the calculation utilized a molar extinction coefficient of 1,400 M⁻¹cm⁻¹ for benzaldehyde [36]. Results were graphed and analyzed in Origin 2023.

Folate binding assays were adapted from previously reported protocols [22, 37]. Briefly, enzyme solutions at 1 mg mL⁻¹ were formulated in the presence of 0 - 40 mM glycine. Each solution was mixed 1:1 with a solution of FTHF in a 96-well plate. The plate was analyzed by absorbance scan (450 - 550 nm) in a BioTek Epoch II plate reader to monitor a peak at ~500 nm, consistent with the formation of the SHMT8•folate complex, as previously reported [37]. The baseline absorbance at 540 nm was subtracted from the absorbance at 500 nm. The working concentrations of glycine tested were 0 – 20 mM. The working concentrations of FTHF tested ranged from 0 – 100 μ M. The data were analyzed by plotting absorbance versus substrate

concentration and were globally fit to the Michaelis–Menten equation, assuming $K_{\rm m} \sim K_{\rm d}$. Data were plotted and analyzed in Origin 2023.

Native gels and limited proteolysis

Native polyacrylamide gel electrophoresis (NativePAGE) was performed using the NativePAGE™ 4-16% Bis-Tris Gel and running buffer kit (Invitrogen by ThermoFisher Scientific). SHMT8 proteins were prepared at 2 mg/mL in 50 mM Hepes, pH 7.5, 150 mM NaCl, and 0.5 mM TCEP. Samples were formulated with 4X NativePAGE™ sample buffer (1M Tris-HCl, 1% Bromophenol Blue, 100% glycerol, pH 6.8) and NativePAGE™ 5% G-250 sample additive, according to the NativePAGE™ Novex® Bis-Tris Gel System protocol by Life technologies (2012). Electrophoresis was performed at 80 V constant for 2 h at room temperature. NativeMark ™ Unstained Protein Standard (ThermoFisher Scientific) was used as the MW marker, and proteins were visualized through Coomassie Brilliant Blue staining for 15 minutes after electrophoresis.

Protein samples at 1.5 mg/ml were incubated with 0.075 mg/mL proteinase K (GoldBio) in 50 mM Hepes, pH 7.5, 150 mM NaCl, and 0.5 mM TCEP at a 200:1 (w/w) ratio. Digestion was conducted at room temperature, aliquots were removed at various time points, and the reaction terminated by the addition of phenylmethylsulfonyl fluoride (final concentration: 3 mM). The reaction mixtures were subject to SDS-PAGE on 14% polyacrylamide gels.

Circular dichroism spectroscopy

CD measurements were conducted with protein samples at concentrations of $\sim 10~\mu M$ prepared in 10 mM potassium phosphate, pH 7.5, and analyzed at 30 °C in a 0.5 mm quartz cuvette using a Chirascan V100 spectrometer (Applied Photophysics) equipped with a multi-cell turret and a Peltier temperature-controlled cell holder. Background subtraction was performed using buffer as a reference. For thermal denaturation, the four protein samples were heated simultaneously from 30 to 70 °C in steps of 5 °C while monitoring ellipticity from 205 to 280 nm. A plot of normalized ellipticity at 222 nm as function of temperature was fitted to the Boltzmann sigmoidal equation to determine the T_m using Origin 2023. As thermal denaturation of SHMT8 is not reversible, the apparent T_m reports on both the thermal stability and the kinetics of unfolding in this system.

Supplementary files

Supplementary figures 1-6.

Supplementary video 1.

Funding

This work was supported by a joint NSF/USDA award IOS 2152548/NIFA 2021-67013-35887 to LJB and MGM. LFO was the recipient of a Wayne L. Ryan fellowship from the University of Missouri Department of Biochemistry. This research used resources of the Advanced Light Source, which is a Department of Energy Office of Science User Facility under contract no. DE-AC02–05CH11231. Some of the data reported here were collected on a Chirascan v100 circular dichroism spectrometer funded by National Institutes of Health grant 1S10OD026703-01.

Acknowledgements

We thank Jay Nix of the Advanced Light Source Beamline 4.2.2 for assistance with X-ray data collection and processing.

Data availability

Materials from this study will be made available from the corresponding author upon reasonable request.

REFERENCES

- Batool, N., Ko, K. S., Chaurasia, A. K. and Kim, K. K. (2020) Functional identification of serine hydroxymethyltransferase as a key gene involved in lysostaphin resistance and virulence potential of staphylococcus aureus strains. *International Journal of Molecular Sciences*, MDPI AG **21**, 1–20 https://doi.org/10.3390/ijms21239135
- 2 Jin, Q., Xie, X., Zhai, Y. and Zhang, H. (2023) Mechanisms of folate metabolism-related substances affecting Staphylococcus aureus infection. *International Journal of Medical Microbiology* **313**, 151577 https://doi.org/10.1016/j.ijmm.2023.151577
- 3 Maenpuen, S., Mee-udorn, P., Pinthong, C., Athipornchai, A., Phiwkaow, K., Watchasit, S., et al. (2023) Mangiferin is a new potential antimalarial and anticancer drug for targeting serine hydroxymethyltransferase. *Archives of Biochemistry and Biophysics* **745**, 109712
- 4 Schwertz, G., Witschel, M. C., Rottmann, M., Bonnert, R., Leartsakulpanich, U., Chitnumsub, P., et al. (2017) Antimalarial Inhibitors Targeting Serine Hydroxymethyltransferase (SHMT) with in Vivo Efficacy and Analysis of their Binding Mode Based on X-ray Cocrystal Structures. *Journal of Medicinal Chemistry* **60**, 4840–4860 https://doi.org/10.1021/acs.jmedchem.7b00008
- 5 Schwertz, G., Witschel, M. C., Rottmann, M., Leartsakulpanich, U., Chitnumsub, P., Jaruwat, A., et al. (2018) Potent Inhibitors of Plasmodial Serine Hydroxymethyltransferase (SHMT) Featuring a Spirocyclic Scaffold. *ChemMedChem* **13**, 931–943 https://doi.org/10.1002/cmdc.201800053
- Witschel, M. C., Rottmann, M., Schwab, A., Leartsakulpanich, U., Chitnumsub, P., Seet, M., et al. (2015) Inhibitors of plasmodial serine hydroxymethyltransferase (SHMT): Cocrystal structures of pyrazolopyrans with potent blood- and liver-stage activities. *Journal of Medicinal Chemistry* **58**, 3117–3130 https://doi.org/10.1021/jm501987h
- 7 Corral, M. G., Leroux, J., Stubbs, K. A. and Mylne, J. S. (2017) Herbicidal properties of antimalarial drugs. *Sci Rep* **7**, 45871 https://doi.org/10.1038/srep45871
- 8 Li, Z., Wang, M., Bai, H., Wang, H., Han, J., An, L., et al. (2024) Serine hydroxymethyl transferase is a binding target of caprylic acid: Uncovering a novel molecular target for a herbicide and for producing caprylic acid-tolerant crops https://doi.org/10.7554/eLife.94853.1
- 9 Ducker, G. S., Ghergurovich, J. M., Mainolfi, N., Suri, V., Jeong, S. K. and Li, S. H. (2017) Human SHMT inhibitors reveal defective glycine import as a targetable metabolic vulnerability of diffuse large B-cell lymphoma. *Proc Natl Acad Sci U S A* **114**, 11404–09 https://doi.org/10.1073/pnas.1706617114
- 10 Geeraerts, S. L., Kampen, K. R., Rinaldi, G., Gupta, P., Planque, M., Louros, N., et al. (2021) Repurposing the antidepressant sertraline as SHMT inhibitor to suppress serine/glycine synthesis—addicted breast tumor growth. *Molecular Cancer Therapeutics* **20**, 50–63 https://doi.org/10.1158/1535-7163.MCT-20-0480
- 11 Giardina, G., Paone, A., Tramonti, A., Lucchi, R., Marani, M., Magnifico, M. C., et al. (2018) The catalytic activity of serine hydroxymethyltransferase is essential for de novo nuclear dTMP synthesis in lung cancer cells. *FEBS Journal*, Blackwell Publishing Ltd **285**, 3238–3253 https://doi.org/10.1111/febs.14610

- 12 Jain, M., Nilsson, R., Sharma, S., Madhusudhan, N., Kitami, T., Souza, A., et al. (2012) Metabolite Profiling Identifies a Key Role for Glycine in Rapid Cancer Cell Proliferation. *Science* **336**, 1040–1045 https://doi.org/10.1126/science.1218595
- 13 Marani, M., Paone, A., Fiascarelli, A., Macone, A., Gargano, M., Rinaldo, S., et al. (2015) A pyrazolopyran derivative preferentially inhibits the activity of human cytosolic serine hydroxymethyltransferase and induces cell death in lung cancer cells 7, 4570–4583 https://doi.org/10.18632/oncotarget.6726.
- 14 Korasick, D. A., Kandoth, P. K., Tanner, J. J., Mitchum, M. G. and Beamer, L. J. (2020) Impaired folate binding of serine hydroxymethyltransferase 8 from soybean underlies resistance to the soybean cyst nematode. *Journal of Biological Chemistry* **295**, 3708–3718 https://doi.org/10.1074/jbc.RA119.012256
- 15 Korasick, D. A., Owuocha, L. F., Kandoth, P. K., Tanner, J. J., Mitchum, M. G. and Beamer, L. J. (2024) Structural and functional analysis of two SHMT8 variants associated with soybean cyst nematode resistance. *The FEBS Journal* 291, 323–337 https://doi.org/10.1111/febs.16971
- 16 Bandara, A. Y., Weerasooriya, D. K., Bradley, C. A., Allen, T. W. and Esker, P. D. (2020) Dissecting the economic impact of soybean diseases in the United States over two decades. *PLoS ONE* **15**, 1–28 https://doi.org/10.1371/journal.pone.0231141
- 17 Kandoth, P. K., Liu, S., Prenger, E., Ludwig, A., Lakhssassi, N., Heinz, R., et al. (2017) Systematic mutagenesis of serine hydroxymethyltransferase reveals an essential role in nematode resistance. *Plant Physiology* **175**, 1370–1380 https://doi.org/10.1104/pp.17.00553
- 18 Liu, S., Kandoth, P. K., Warren, S. D., Yeckel, G., Heinz, R., Alden, J., et al. (2012) A soybean cyst nematode resistance gene points to a new mechanism of plant resistance to pathogens. *Nature*, Nature Publishing Group **492**, 256–260 https://doi.org/10.1038/nature11651
- 19 Jabs, A., Weiss, M. S. and Hilgenfeld, R. (1998) Non-proline Cis Peptide Bonds in Proteins. *J Mol Biol* **286**, 291–304 https://doi.org/10.1006/jmbi.1998.2459
- Weiss, M. S., Jabs, A. and Hilgenfeld, R. (1998) Peptide bonds revisited. *Nat Struct Mol Biol* **5**, 676–676 https://doi.org/10.1038/1368
- 21 Das, S., Ramakumar, S. and Pal, D. (2014) Identifying functionally important *cis* -peptide containing segments in proteins and their utility in molecular function annotation. *The FEBS Journal* **281**, 5602–5621 https://doi.org/10.1111/febs.13100
- 22 Florini, J. R. and Vestling, C. S. (1957) Graphical determination of the dissociation constants for two-substrate enzyme systems. *BBA Biochimica et Biophysica Acta* **25**, 575–578 https://doi.org/10.1016/0006-3002(57)90529-2
- 23 Jala, V., Appaji Rao, N. and Savithri, H. (2003) Identification of amino acid residues, essential for maintaining the tetrameric structure of sheep liver cytosolic serine hydroxymethyltransferase, by targeted mutagenesis. *Biochem J* 369, 469–476 https://doi.org/10.1042/BJ20021160
- 24 Krishna Rao, J. V., Jagath, J. R., Sharma, B., Appaji Rao, N. and Savithri, H. S. (2015) Asp-89: a critical residue in maintaining the oligomeric structure of sheep liver cytosolic serine hydroxymethyltransferase. *Biochemical Journal* **343**, 257–263 https://doi.org/10.1042/bj3430257
- Zanetti, K. A. and Stover, P. J. (2003) Pyridoxal phosphate inhibits dynamic subunit interchange among serine hydroxymethyltransferase tetramers. *Journal of Biological Chemistry* 278, 10142–10149 https://doi.org/10.1074/jbc.M211569200

- Lakhssassi, N., Patil, G., Piya, S., Zhou, Z., Baharlouei, A., Nguyen, H. T., et al. (2019) Genome reorganization of the GmSHMT gene family in soybean showed a lack of functional redundancy in resistance to soybean cyst nematode. *Scientific Reports* 9, 1–16 https://doi.org/10.1038/s41598-018-37815-w
 Fu, T., Boja, E. S., Safo, M. K. and Schirch, V. (2003) Role of Proline Residues in the
- 27 Fu, T., Boja, E. S., Safo, M. K. and Schirch, V. (2003) Role of Proline Residues in the Folding of Serine Hydroxymethyltransferase. *J Biol Chem* 278, 31088–31094 https://doi.org/10.1074/jbc.M303779200
- 28 García-Cazorla, À., Verdura, E., Juliá-Palacios, N., Anderson, E. N., Goicoechea, L., Planas-Serra, L., et al. (2020) Impairment of the mitochondrial one-carbon metabolism enzyme SHMT2 causes a novel brain and heart developmental syndrome. *Acta Neuropathol* **140**, 971–975 https://doi.org/10.1007/s00401-020-02223-w
- 29 Majethia, P., Bhat, V., Yatheesha, B. L., Siddiqui, S. and Shukla, A. (2022) Second report of SHMT2 related neurodevelopmental disorder with cardiomyopathy, spasticity, and brain abnormalities. *European Journal of Medical Genetics* **65**, 104481 https://doi.org/10.1016/j.ejmg.2022.104481
- 30 Kabsch, W. (2010) Software XDS for image rotation, recognition and crystal symmetry assignment. *Acta Crystallogr., Sect. D: Biol. Crystallogr.* **66**, 125–132 https://doi.org/10.1107/S0907444909047337
- 31 Winn, M. D., Ballard, C. C., Cowtan, K. D., Dodson, E. J., Emsley, P., Evans, P. R., et al. (2011) Overview of the CCP4 suite and current developments. *Acta Crystallographica Section D: Biological Crystallography* **67**, 235–242 https://doi.org/10.1107/S0907444910045749
- 32 Adams, P. D., Afonine, P. V., Bunkóczi, G., Chen, V. B., Davis, I. W., Echols, N., et al. (2010) PHENIX: A comprehensive Python-based system for macromolecular structure solution. *Acta Crystallographica Section D: Biological Crystallography* **66**, 213–221 https://doi.org/10.1107/S0907444909052925
- 33 Emsley, P. and Cowtan, K. (2004) Coot: Model-building tools for molecular graphics. *Acta Crystallographica Section D: Biological Crystallography* **60**, 2126–2132 https://doi.org/10.1107/S0907444904019158
- 34 DeLano, W. L. (2002) The PyMOL Molecular Graphics System
- 35 Krissinel, E. and Henrick, K. (2007) Inference of Macromolecular Assemblies from Crystalline State. *Journal of Molecular Biology* **372**, 774–797 https://doi.org/10.1016/j.jmb.2007.05.022
- 36 Chiba, Y., Terada, T., Kameya, M., Shimizu, K. and Arai, H. (2012) Mechanism for folate-independent aldolase reaction catalyzed by serine hydroxymethyltransferase. *FEBS Journal* **279**, 504–514 https://doi.org/10.1111/j.1742-4658.2011.08443.x
- 37 Schirch, L. and Ropp, M. (1967) Serine transhydroxymethylase. Affinity of tetrahydrofolate compounds for the enzyme and enzyme-glycine complex. *Biochemistry* **6**, 253–7 https://doi.org/10.1021/bi00853a039

Table 1. X-ray data collection and refinement statistics.

	E.P285S	F.P285S*
Wavelength (Å)	0.9999	1.0000
Resolution range (Å)	40.75 - 2.25 (2.33 - 2.25)	48.5 - 1.9 (1.97 - 1.9)
Space group	$P \ 2_1 \ 2_1 \ 2$	$P 3_1 2 1$
Unit cell (Å)	a=116.60 b=129.69 c=58.63	a=174.18 c=183.66
Observations	585,798 (59164)	2,611,750 (248617)
Unique reflections	42,995 (4236)	251,545 (24819)
Multiplicity	13.6 (14.0)	10.4 (10.0)
Completeness (%)	99.86 (99.76)	99.71 (99.62)
Mean I/σ(I)	15.62 (0.94)	13.95 (1.60)
$R_{ m merge}$	0.1048 (2.812)	0.157 (1.702)
R_{pim}	0.02953 (0.7779)	0.05119 (0.5648)
$\overrightarrow{\mathrm{CC}}_{1/2}$	0.999 (0.594)	0.997 (0.587)
$R_{ m work}$	0.1951 (0.3682)	0.2304 (0.4627)
$R_{ m free}$	0.2585 (0.4270)	0.2674(0.4770)
No. of non-H atoms	7038	21398
macromolecules	6786	20533
ligand atoms (Lys-PLP)	132	396
solvent	252	865
Protein residues	902	2716
rmsd bonds (Å)	0.016	0.008
rmsd angles (°)	1.44	0.99
Ramachandran favored (%)	95.34	96.99
Ramachandran allowed (%)	4.55	2.94
Ramachandran outliers (%)	0.11	0.08
Rotamer outliers (%)	1.19	0.69
Clashscore	9.54	4.65
Average B-factor	67.30	40.23
macromolecules	67.44	40.32
solvent	63.70	38.12
PDB ID	9CE6	9CG8

Statistics for the outer resolution shell are shown in parentheses.

^{*}Data set affected by translational non-crystallographic symmetry, likely contributing to somewhat high $R_{\rm free}$.

FIGURES

Figure 1. An overview of the tetramer of soybean SHMT8, the isomers of proline, and schematic of ligand binding residues. (A) The tetramer of SHMT8 (PDB ID 6UXJ) with the four polypeptide chains shown in different colors (dark teal, pink, purple, and light blue). The PLP cofactor is yellow and the substrate analog FTHF is green. Pro285 is red. (B) The trans and cis stereoisomers of proline. (C) A schematic highlighting key ligand binding residues on the sequence of SHMT8. Contacting residues are shown above the sequence and color-coded as follows: blue lines – PLP-Gly; green lines – FTHF; orange lines: both PLP-Gly and FTHF. The cis-proline (P285) and active site lysine that forms a covalent linkage to PLP (Lys244) are highlighted with triangles under the sequence. The two residue variants associated with SCN-resistance in Forrest SHMT8 are shown by yellow bars. Enzyme-ligand contacts determined from PDB ID 6UXJ.

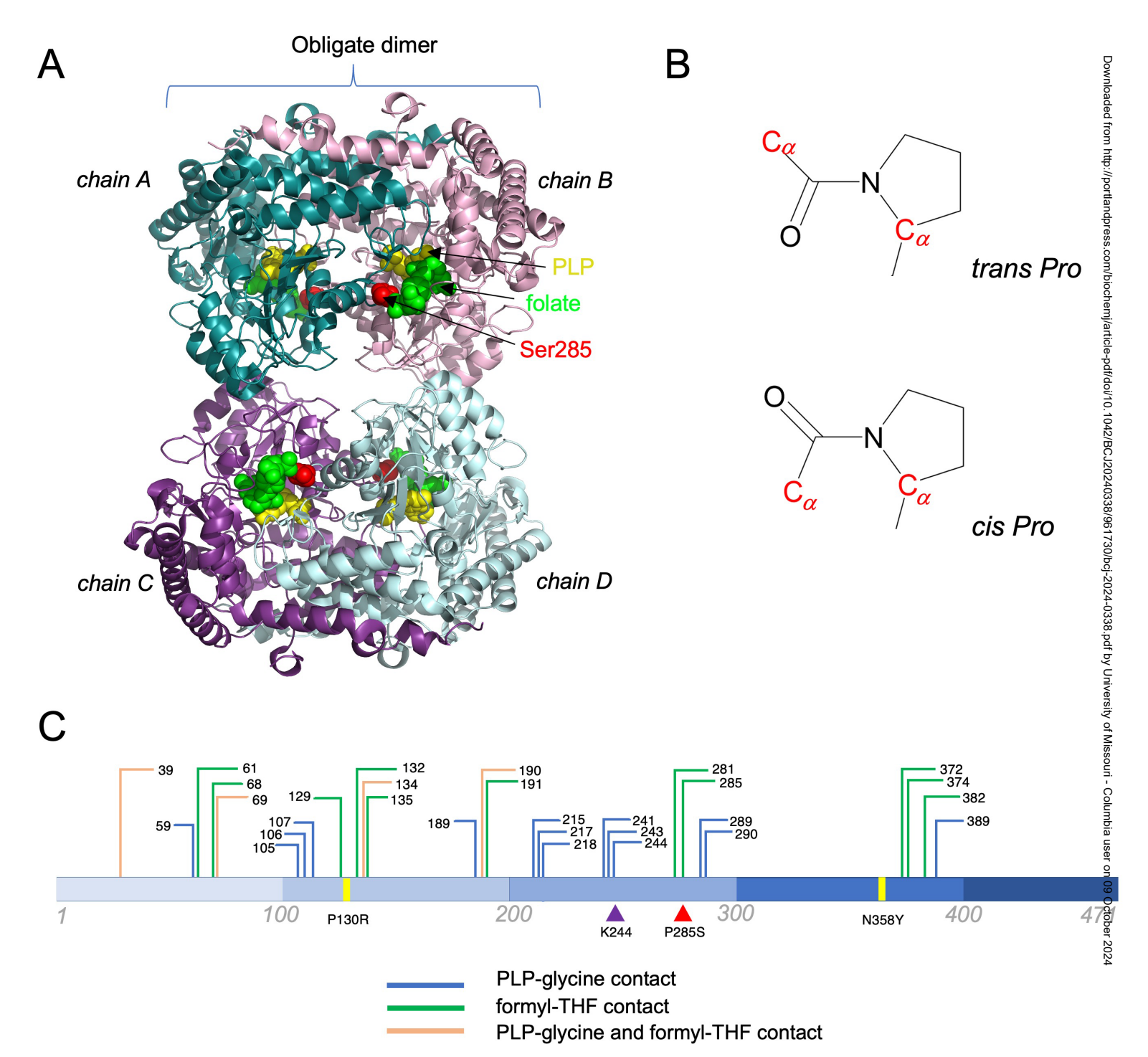
Figure 2. Structural context of Pro285 in SHMT8 (PDB ID 6UXH). (A) The two protomers of one obligate dimer are in pink and dark cyan. PLP and Pro285 are in a space filling model. (B) View of obligate dimer 90° from A). (C) Schematic of the obligate dimer highlighting the proximity of Pro285 from chain A to the PLP bound to chain B, and vice versa.

Figure 3. Structural impacts of the P285S mutation on SHMT8. (A) An overview of the E.P285S tetramer highlighting regions of structural change near the tetramer interface (dashed line). Ser285 is in red and the PLP internal aldimine in its altered binding pose is yellow. The native conformation of the polypeptide chain (residues 128-147) is overlaid (blue); this region is

altered/disordered in the mutant. (B) A close-up view of residue 285 in a superposition of the Essex SHMT8 complex with PLP (PDB ID 6UXH, dimer chains in teal/pink) and the E.P285S mutant (dimer in gray/beige). The binding pose of PLP (yellow) in Essex SHMT8 is reoriented in the E.P285S mutant (PLP in orange). The displacement of a turn region in E.P285S that invades the PLP binding site is highlighted by red arrow. (C) A close-up view showing selected enzyme hydrogen bonds to the PLP-Gly reaction intermediate, as seen in the complex with Essex SHMT8 (6UXI; green). The glycine part of the ligand is highlighted by green label; PLP in the E.P285S is superimposed (semi-transparent in orange) to show how its phosphate group localizes to the position of the glycine in PLP-Gly. (D) Enzyme hydrogen bonds with PLP internal aldimine in its altered binding pose in the structure of the E.P285S mutant. Only one direct contact to Arg389 (chain B) and one water-mediated contact to Tyr59 (chain A) are present between the enzyme and ligand.

Figure 4. Native gel electrophoresis and limited proteolysis studies of Essex and Forrest SHMT8, and their respective P285S mutants. (A) Native polyacrylamide gel electrophoresis of SHMT8 proteins, showing increase in the relative amounts of dimer compared to tetramer for the P285S mutants. NativePAGE molecular weight markers were used (see Methods). (B, C) Limited proteolysis of the same proteins showing a general increase in susceptibility of the P285S variants relative to Essex/Forrest SHMT8. Forrest SHMT8 also shows some changes in proteolysis relative to Essex SHMT8 presumably related to the P130R/N358Y polymorphisms.

Figure 1



Blochemical Journal. This is an Accepted Manuscript. You are encouraged to use the Version of Record that, when published, will replace this version. The most up-to-date-version is available at https://doi.org/10.1042/BCJ20240338

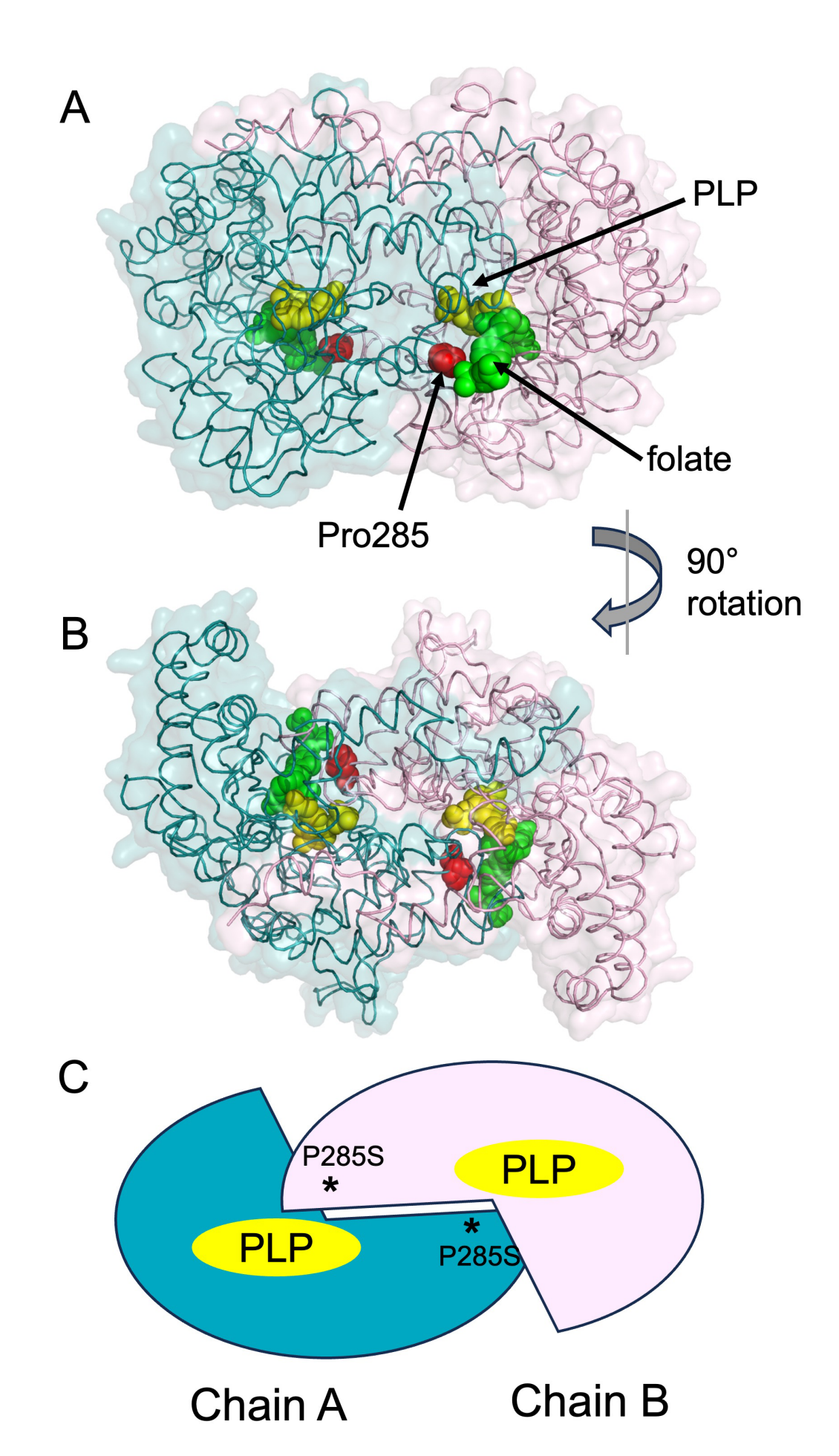


Figure 3

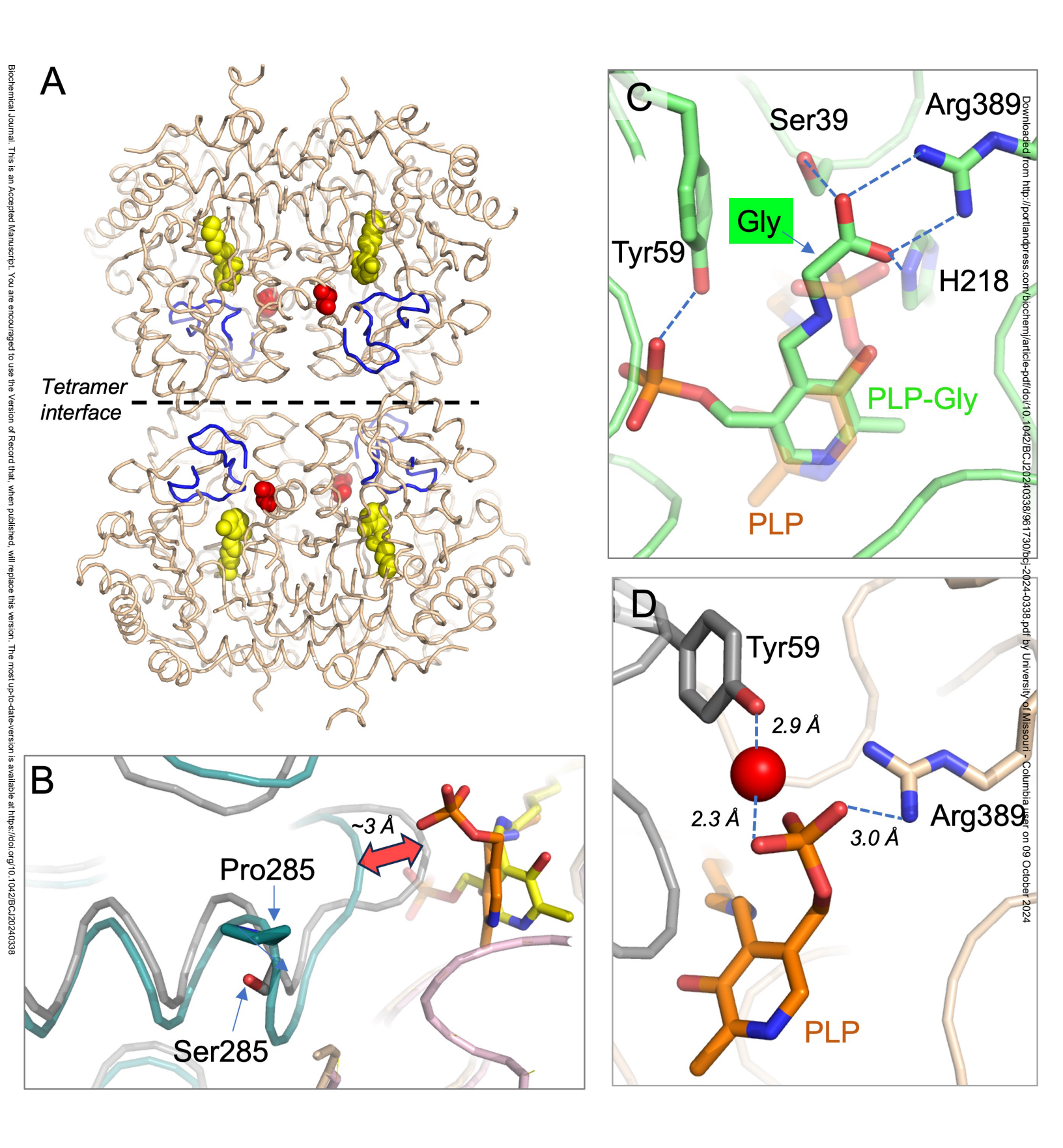


Figure 4

